


# Efficient Shortcut Method for Determining the Process Window in Stirred-Pulsed Extraction Columns

Mira Schmalenberg\*, Timothy Aljoscha Frede, Christopher Mathias, and Norbert Kockmann

DOI: 10.1002/cite.202000066

 This is an open access article under the terms of the Creative Commons Attribution License, which permits use, distribution and reproduction in any medium, provided the original work is properly cited.

Recent studies showed the superior separation performance of stirred-pulsed columns of different diameters in liquid-liquid extraction processes. Here, an efficient shortcut method will be presented, which is time and resource-efficient as well as cost-effective to determine the operational window of these columns for industrial separation tasks. Savings in time of less experiments and costs of materials consumption can be estimated with up to 30 %. The presented method is particularly suitable before the application of new chemical systems, which are particularly cost-intensive and scarce in material supply.

**Keywords:** Flooding point determination, Liquid-liquid extraction, Shortcut design method, Small-scale extraction column, Stirred-pulsed extraction column

*Received:* April 01, 2020; *accepted:* December 18, 2020

## 1 Introduction

Liquid-liquid extraction is an essential thermal separation technique with many applications in petrochemistry or biochemical and pharmaceutical industry. Three major categories of extraction apparatus are mixer-settlers, rotary extractors, or columns. The latter make use of the density difference between the extract and raffinate phases so that they can be operated in countercurrent operation. Further subdivisions are made with regard to the mechanical energy input with stirring or pulsation. A detailed overview of different column types can be found in the literature [1–3] and should not be presented here.

The stirred-pulsed liquid-liquid extraction columns with internal diameters of DN15, DN32, and DN50 have already been characterized with the standard material system butyl-acetate/acetone/water [4–6], which is recommended by the European Federation of Chemical Engineering (EFCE) [7]. With these results, investigating industrial chemical systems is the next step. Particularly the hydrodynamic behavior of very complex substance systems with several impurities, as they often occur in industry, are difficult to predict, although many thermodynamic models [8, 9] or models using neural networks [10–12] have already been developed.

In this contribution, a practical shortcut method is presented for the application of industrial chemical systems in stirred-pulsed extraction columns to achieve reasonable results in short time with low effort. For this purpose, the industrial system containing salts, impurities, and expensive products are replaced by model component systems in a

first step. By using the model systems, the flooding and hydrodynamic behavior is investigated in a DN15 stirred-pulsed measurement cell and a DN15 stirred-pulsed extraction column. These investigations help finding the optimal operation window for complex industrial chemical systems in a resource-efficient manner. These savings will also be demonstrated.

## 2 Theoretical Background

The performance of an extraction column is mainly defined by volumetric throughput and separation efficiency. The flooding point defines the maximum throughput and thus, the upper limit for the operation window, at which extraction columns cannot be operated properly anymore. At this point, the counter-current flow breaks down and an intense coalescence takes place, which is called phase inversion. The loading  $B$  indicates the throughput of extraction columns and is defined as the total ingoing volume flow rate related to the cross-sectional area of the active extraction part (Eq. (1)). The flooding loading  $B_{\text{flood}}$  refers to the operating state where flooding occurs [3].

---

Mira Schmalenberg, Timothy Aljoscha Frede, Christopher Mathias, Prof. Dr.-Ing. Norbert Kockmann

Mira.Schmalenberg@tu-dortmund.de  
TU Dortmund University, Department of Biochemical and Chemical Engineering, Laboratory of Equipment Design, Emil-Figge-Straße 68, 44227 Dortmund, Germany.

$$B = \frac{\dot{V}_{\text{dis,in}} + \dot{V}_{\text{conti,in}}}{A_{\text{active}}} \quad (1)$$

As a rule of thumb, the column should be operated at 80 % of the flooding loading to maximize the separation performance at high throughput [3]. This operating point is denoted with  $B_{80}$ . The prediction of flooding points is difficult due to the large number of influencing parameters such as concentration, temperature, impurities, stirrer speed and pulsation. Thus, correlations from literature are often not transferable to other chemical systems and column geometries [13, 14].

The drop size is a crucial factor of two-phase flow within the column. In practice, there is a size distribution of different drop sizes in a dispersion, which can be represented by the Sauter mean diameter  $d_{32}$ . The Sauter mean diameter is defined as the diameter of drops, which has the same surface-to-volume ratio ( $S_{\text{tot}}V_{\text{tot}}^{-1}$ ) as the whole droplet size distribution (Eq. (2)).

$$d_{32} = \frac{6 \cdot V_{\text{tot}}}{S_{\text{tot}}} \quad (2)$$

The mean diameter is an indicator for separation performance and flooding limit and can be determined in glass-wall columns. In order to increase the extraction performance, narrow droplet size distributions are favorable [13, 15]. Very small droplets can lead to low column loading, although in general, small droplets increase the mass transfer rate [6]. In the literature, for example, a Sauter diameter of 1.5–2.5 mm in extraction columns is recommended as a proper droplet size [3].

### 3 Materials and Methods

#### 3.1 Experimental Setup of Extraction Equipment

The DN15 measurement cell representing the stirred-pulsed extraction column consists of an active extraction part made of glass with cooling jacket for precise temperature control. The length of the active part is 136 mm for six stirrers separated by perforated plates [4]. The plates divide the active extraction part in six compartments with a height of 20 mm each. Thus, the active volume of the measurement cell is 19 mL. The pulsation unit is directly flange-mounted to the bottom part of the measurement cell.

In contrast to the DN15 measurement cell, the DN15 extraction column additionally has a head and a bottom for phase separation. The structure of the internals is the same as for the measurement cell. Due to the higher length of the active extraction part of 220 mm, the number of compartments is increased to ten. The extraction column setup has been described in detail in previous works of Soboll et al. [5, 6]. A detailed comparison of both extraction devices is given in Tab. 1 with main geometrical dimensions. The sys-

**Table 1.** Comparison of DN15 measurement cell and DN15 column.

Property	DN15 measurement cell	DN15 column
Number of stirrer compartments [-]	6	10
Length of active extraction part [mm]	136	220
Volume of active extraction part [mL]	19	32
Total volume [mL]	27	233

tem periphery of both apparatuses is described and illustrated (Fig. 1) in the following.

Micro annular gear pumps (MZR-7255, HNP Mikrosysteme, Germany) are used to feed the liquid streams of organic solvent and aqueous mixture into the measurement cell. The rotational speed of these pumps is controlled via Coriolis flow meters (Mini Cori-Flow, Bronkhorst, Netherlands). A syringe pump (SyrDos 2, HiTec Zang, Germany) is used to adjust the outlet flow rate of the heavy phase. The light, organic phase leaves the measurement cell via overflow at the head of the column. Mass flow rates of ingoing aqueous and organic phase are equal. A thermostat (Minichiller, Huber, Germany) provides cooling water for the jacket of the measurement cell and the heat exchangers to preheat the ingoing liquids.

Pulsation of the liquid within the measurement cell is induced through periodic, reciprocating motion of a stainless piston driven by a double acting pneumatic cylinder. The piston-cylinder system is connected by a tube to the bottom of the measurement cell. The stroke length (peak-to-peak amplitude) of the pulsation movement is 6 mm inside the active extraction part. The time periods for upward and downward stroke are equal without any stop times, resulting in a motion profile that corresponds to a triangle wave.

Sieve plates serve as stators and divide the active extraction part into compartments. There are 12 holes in the sieve plates, each with a diameter of 2 mm. The compartment height is 20 mm. There is one six-blade stirrer with 5 mm height in each compartment, while all stirrers are mounted on a central shaft. All column internals are made of stainless steel.

The setup of the DN15 column is almost similar to that of the measurement cell. The peripheral equipment differs at some points. The jacket of the column is heated using a thermofluid (DW-Therm M90.200.02, Huber, Germany) and a thermostat (Ministat 240, Huber, Germany). The ingoing liquids are preheated using an oil bath, which is connected to the thermostat, and fed into the column using gear pumps (BVP-Z, Ismatec, Germany). The mass flow rates of these pumps are calibrated before each experiment. The outlet of the aqueous phase is controlled with an overflow construction.

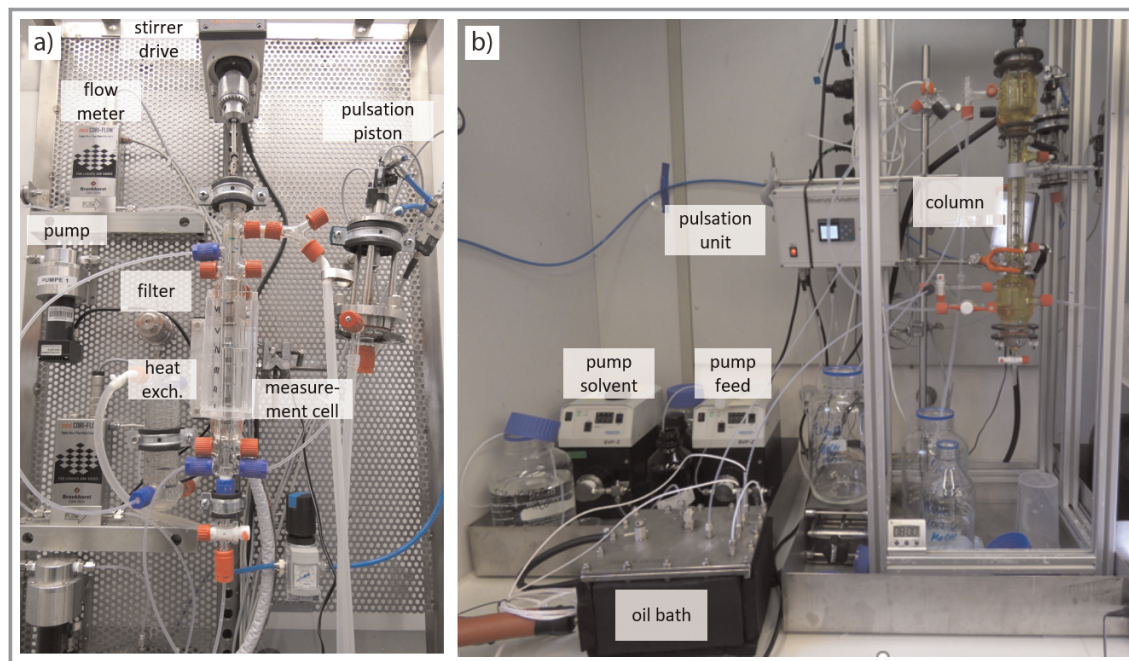


**Figure 1.** a) Extraction DN15 measurement-cell and its assembly. b) Extraction DN15 column and its assembly.

### 3.2 Chemicals

The shortcut method is tested with two industrial systems A and B, which are provided by the industrial partner Merck KGaA. Both systems consist of carrier liquid, product, solute and impurities. Carrier liquid of system A and B is n-heptane and toluene, respectively. The solutes are catalysts, which were added during the reaction step to form the products. The industrial systems are always the dispersed, light phase while the solvent is the continuous, heavy phase. A mixture of methanol (>99.9%, Merck KGaA, Germany) and water (deionized, electrical conductivity  $\leq 5 \cdot 10^{-4} \text{ S m}^{-1}$ ) is used as solvent for system A, water and a complexing agent (>99.0%, Merck KGaA, Germany) for system B. Correspondingly, model system A is n-heptane (>99%, Merck KGaA, Germany)/methanol-water mixture (50 wt% each). Model system B is toluene (>99.0%, Merck KGaA, Germany)/water.

### 3.3 Determination of Flooding Point

The flooding point is determined for different stirrer speeds (500, 700, 800, and 900 rpm) and different pulsation frequencies (0.5, 1.0, and 1.5 Hz). The lowest flooding loading is expected for the highest stirrer speed and lowest pulsation frequency, see [4]. Thus, the flooding point determination starts with this combination of operating parameters (here 900 rpm and 0.5 Hz). At first, the column is started by filling with the heavy aqueous phase. The total mass flow rate of both components (feed and solvent) is increased succes-

sively by  $2 \text{ g min}^{-1}$  from starting flow rate of an already investigated system (here  $10 \text{ g min}^{-1}$  for each phase) and the two-phase flow is observed for 15 min. This procedure is continued until flooding behavior is detected.

The next flooding point is determined at the next lower stirrer speed and constant pulsation frequency. Therefore, the total mass flow rate of the previous determination is slightly reduced by  $4 \text{ g min}^{-1}$  in total. Here again, the total mass flow rate is successively increased until flooding behavior is detected. This procedure is repeated for different stirrer speeds at a constant pulsation frequency until the next higher pulsation frequency is set. Pulsation amplitude is always 6 mm. The first flooding point of this measuring sequence is determined at the highest stirred speed. The starting point is the total mass flow rate of the flooding point with same stirred speed and next lower pulsation frequency reduced by  $2 \text{ g min}^{-1}$  in total. A schematic overview of the method is given in Fig. 2a.

### 3.4 Shortcut Method to Determine Flooding Points for Industrial Liquid-liquid Systems

The identification of the operation window of industrial systems in extraction columns is time and cost consuming [16,17]. The following method is an approach to reduce consumption of chemicals by minimizing the number of potential flooding points during the identification of the operation window. Therefore, flooding points of the industrial systems are estimated based on hydrodynamic studies of a reduced form of the industrial system, the so-called

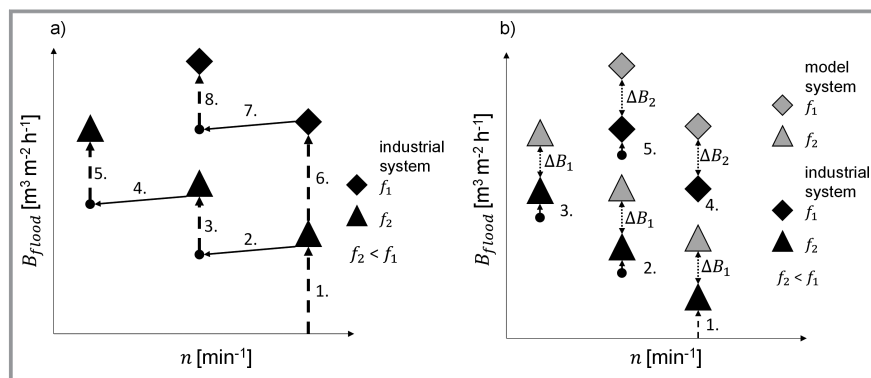


**Figure 2.** a) Schematic representation of the conventional method. b) Schematic representation of the shortcut method.

model system. The model system consists only of the carrier liquid of the industrial feed stream and the solvent.

In a first step, the dependency of the flooding loading on stirrer speed and pulsation frequency of the model system is investigated (as described in Sect. 3.2). Subsequently, the flooding points of the industrial system are determined analogously.

### 3.5 Determination of Drop Size

Drop sizes are determined by taking digital images of the dispersion taken with a digital camera (iPhone 6S, Apple Inc., USA) at  $B_{80}$  to exclude flooding during the experiments and ensure stable two-phase flow. An acrylic glass box is placed around the active extraction part and filled with deionized water to reduce optical distortions caused by the cylindrical shape of the column [18]. In the back of the acrylic glass box, a LED panel (StarCluster 3270, Kaiser Fototechnik, Germany) is placed for illumination. The droplet sizes are determined by measuring drop diameters manually using the software ImageJ<sup>®</sup>. For a sufficient statistic, at least 300 droplets are counted per operating point. Sauter mean diameter is calculated with Eq. (2) and serves as indicator for mass transfer, separation efficiency and limit for flooding.

## 4 Results and Method Development

In the following, a comparison of the flooding loadings in the different apparatuses (measurement cell and column) is carried out. In particular, the difference of the flooding loadings between the model system and the industrial

substance system is analyzed in order to evaluate the presented shortcut method on the basis of these results. Furthermore, a comparison of the droplet Sauter diameters between measurement cell and column at  $B_{80}$  follows to illustrate the comparability of these two apparatuses.

### 4.1 Flooding Points

#### 4.1.1 System A

Flooding loadings of model and industrial system A in DN15 measurement cell are shown as function of stirrer speed at fixed pulsation frequencies in Fig. 3a.

In general, flooding loadings decrease with higher stirrer speed and increase with higher pulsation frequency, thus, indicating typical trends for stirred extraction columns [19]. Lower flooding loadings of the industrial system are due to the influence of various components, which reduce the density difference between solvent and disperse phase. This results in a lower buoyancy force of the droplets, hence, the droplets accumulate and the column floods at lower loadings. Furthermore, flooding of the systems was investigated for different stirrer speeds and pulsation frequencies in the DN15 column (Fig. 3b).

Flooding curves show the same trend, in which higher frequencies and lower stirrer speeds lead to higher flooding loadings. In addition, the stirrer speed dependence increases with increasing pulsation frequency for both systems. It can also be seen that the flooding loadings of the industrial system are lower than those of the model system. Here, the flooding loading differences between the model system and the industrial system are significantly higher than those in the measurement cell. Flooding loadings of the column are above those of the measurement cell at the respective

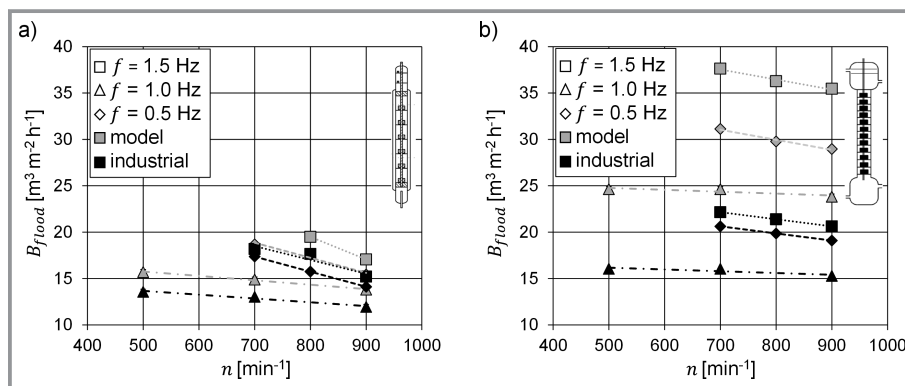


**Figure 3.** a) Flooding loading of model and industrial system A in DN15 measurement cell as function of stirrer speed for different pulsation frequencies. b) Flooding loadings of system A in DN15 column as function of stirrer speed for different pulsation frequencies.



pulsation frequency. This may be caused by differences in apparatus configuration between both setups. Firstly, the inlet zone of the disperse phase occupies a smaller proportion in the column due to the comparatively greater length of the extraction part. Thus, constant flow profile and stable droplet size are obtained earlier than in the measurement cell. Secondly, the liquid hold-up in the column is higher due to the longer extraction section, which results in higher loadings.

#### 4.1.2 System B

Fig. 4 shows the flooding tests for model and industrial system B in the DN15 column as a function of stirrer speed for different pulsation frequencies.

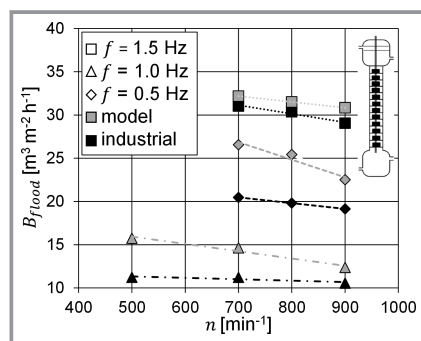


**Figure 4.** Flooding loadings of system B in DN15 column as function of stirrer speed for different pulsation frequencies.

With model and industrial system A, the course of the flooding loadings with increasing stirrer speed is due to decreasing droplet sizes and their higher tendency to coalesce. In particular for the pulsation frequencies  $f = 0.5$  Hz and  $f = 1.0$  Hz, the dependence of the flooding loading on the stirrer speed is stronger for the model system than for the industrial system. In general, flooding loadings of system B are smaller than those of system A, which is due to larger droplets of system B. This favors the accumulation of droplets in the compartments and results in earlier flooding of the column.

#### 4.2 Shortcut Method and Its Applicability

For testing the applicability of the shortcut method, the difference between the flooding loadings  $\Delta B$  is evaluated. Finally, the application of  $\Delta B$  is verified as a shortcut parameter for the estimation of flooding points based on model systems. A schematic overview of the method is given in

Fig. 2b. The difference between the flooding loadings of the model and industrial system is evaluated for different stirrer speeds and pulsation frequencies (Fig. 5).

The almost constant course of the differences, related to the stirrer speed, shows that the flooding behavior of the industrial system can be estimated with sufficient accuracy as soon as flooding curves of the model systems have been determined and a single additional measurement of the flooding point was made for the industrial system. Due to the linear course of the differences, it is possible to predict the flooding loading of the industrial system for a specific pulsation frequency over the investigated area.

The comparison of the conventional and shortcut method is carried out by means of the number of investigated flooding points and the resulting chemical use in both methods. Cost accounting is performed based on the mass flow rates, which were fed during the experiments and the corresponding costs for chemicals. Each operating point, and thus potential flooding point is run for 15 min to ensure steady state of the column. The total costs for the model system  $C_{\text{Model}}$  depend on the time until steady state is reached  $t$  [s], mass flow rate of the solvent  $\dot{m}_S$  [ $\text{kg s}^{-1}$ ] and the carrier liquid  $\dot{m}_C$  [ $\text{kg s}^{-1}$ ], and their corresponding cost  $P_S$  [ $\text{€ kg}^{-1}$ ] and  $P_C$  [ $\text{€ kg}^{-1}$ ], cf. Eq. (3). Total costs for the industrial system are calculated analogously except that the value of the product  $P_P$  [ $\text{€ kg}^{-1}$ ], which the mass flow of the feed  $\dot{m}_F$  [ $\text{kg s}^{-1}$ ] contains, is considered. Therefore, the weight fraction of the carrier liquid  $w_C$  [ $\text{kg kg}^{-1}$ ] and the product  $w_P$  [ $\text{kg kg}^{-1}$ ] are taken into account (Eq. (4)).

$$C_{\text{Model}} = t(\dot{m}_S P_S + \dot{m}_C P_C) \quad (3)$$

$$C_{\text{Industrial}} = t(\dot{m}_S P_S + \dot{m}_F (w_C P_C + w_P P_P)) \quad (4)$$

Subsequently, the economic efficiency of the shortcut method using flooding loading difference as parameter is investigated. Due to sensitivity of the data regarding the costs for chemicals, a percentage of the cost comparison of

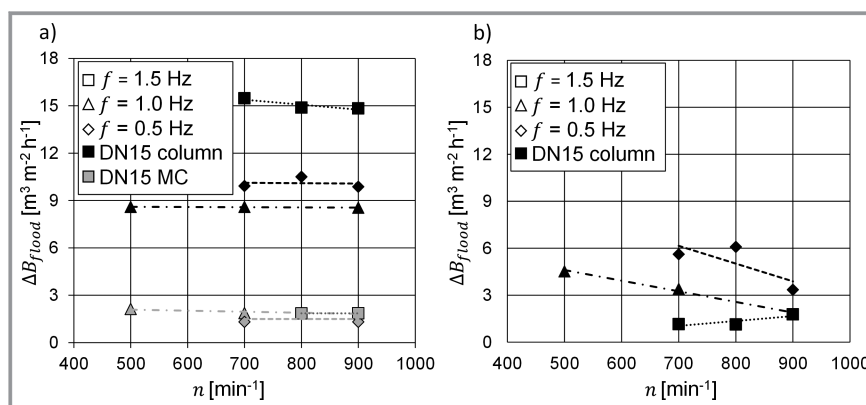


**Figure 5.** a) Flooding loading difference between model and industrial system A in DN15 column and DN15 measurement cell as function of stirrer speed for different pulsation frequencies. b) Flooding loading difference between model and industrial system B in DN15 column as function of stirrer speed for different pulsation frequencies.

both methods is given. The costs for determining all flooding points of the industrial system in the DN15 measurement cell are approximately 30 % higher than using the shortcut method for estimation and verification. In the DN15 column, the costs are approximately 19 % higher. For specific flooding points the cost saving ranges between 3 and 28 %, depending on pulsation frequency. The proportion of cost incurred in determining the flooding points of the model system in the shortcut method is approximately 3 % of the total cost in the DN15 measurement cell and 4 % in the DN15 column, respectively. The cost savings are the result of less operating points that have to be investigated as potential flooding points. The number of potential flooding points is reduced by 12 in the DN15 measurement cell and 7 in the DN15 column, respectively. This leads to lower consumption of operating resources and consequently lower costs. Product material saving ranges between 5 and 34 %, depending on the pulsation frequency. Furthermore, the reduction of potential flooding points also leads to time savings. Thus, especially the experimental data of the DN15 measurement cell provide a fast and comparatively inexpensive basis for estimating flooding points of industrial systems. Calculation of economic efficiency for industrial system B is only possible through a comparison with industrial system A due to the unknown composition. The value of the product in industrial system B is approximately 8 times higher than that of industrial system A. Therefore, it can be assumed that the application of the shortcut method has higher economic efficiency than the conventional method for system B as well.

### 4.3 Droplet Size in Measurement Cell and Extraction Column

Fig. 6 shows the dependency of the Sauter mean diameter of model and industrial system A on the stirrer speeds for fixed pulsation frequencies in DN15 measurement cell and column.

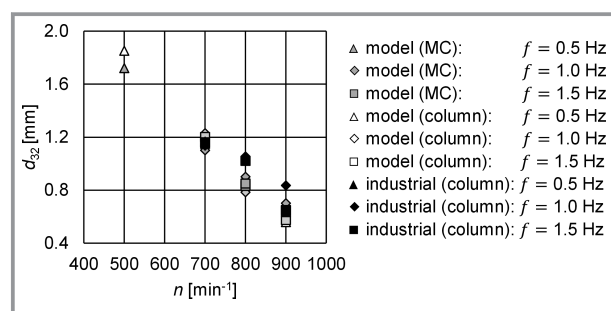


**Figure 6.** Sauter mean diameter of model and industrial system A in DN15 measurement cell and column at different pulsation frequencies depending on stirrer speed at  $B_{80}$ .

Sauter mean diameter decreases linearly with increasing stirrer speed due to increasing shear stress acting on the droplets. The disperse phase is contacted more frequently

per unit of time with the stirrer blades at higher stirrer speeds, which results in a greater dispersion of the droplets. The curves lie for different frequencies on top of each other and exhibit almost identical slopes. This indicates a lower influence of the pulsation frequency on the droplet size than the stirrer speed. Droplet sizes of the industrial system are slightly larger at higher stirrer speeds than those of the model system. In addition, droplet sizes of the model system in the DN15 measurement cell and DN15 column are approximately the same due to the unchanged stirrer and plate geometry. Droplet size is also influenced by physical properties of the chemical system. The assumed decrease of the interfacial of the industrial system, compared to the model system, theoretically leads to smaller droplet sizes. This behavior is not observed here. Hence, the decrease of the density difference, which leads to larger droplets, influences the droplet size of the industrial system stronger than the decrease of the interfacial tension. Optical measurement of droplet size can lead to estimation of separation performance. Droplets smaller than 0.5 to 1 mm have a low flooding velocity and are prone to form emulsions leading to flooding of the column [3, 20, 21].

## 5 Conclusion

An efficient shortcut method was presented to determine the flooding behavior of a new, unknown industrial liquid-liquid extraction system for a stirred-pulsed extraction column or measurement cell in a cost-effective and resource-efficient manner. For this purpose, the flooding points of two industrial systems were each examined with an associated simplified model system, and their flooding loading differences were determined. Since the difference in flooding loadings between the model and the industrial system remains constant at different stirrer speeds and specific pulsation frequency, material savings of up to 34 % can be achieved using this method. Furthermore, the droplet size in an extraction column was compared with the droplet size in a measurement cell (without head and bottom) and it was found that this measured variable can already be well mapped in the measurement cell. Droplet size can serve as indicator for separation efficiency. This hypothesis will be tested in future investigations.

The German Federal Ministry for Economic Affairs and Energy (BMWi) is acknowledged for funding this research as part of the ENPRO2.0 initiative (Support code: 03ET1528A). We acknowledge Dortmund University within the funding programme Open Access Publishing. The authors would also like to thank our technician Carsten Schrömges and the support from Merck KGaA, especially Judit Wenger, Simon Durickij and the technicians from PM-OPE. Open access funding enabled and organized by Projekt DEAL.

## Symbols used

$A$	$[\text{m}^2]$	area
$B$	$[\text{m}^3 \text{m}^{-2} \text{h}^{-1}]$	loading
$C$	$[\text{€ kg}^{-1}]$	total cost
$d_{32}$	$[\text{m}]$	Sauter mean diameter
$f$	$[\text{Hz}]$	pulsation frequency
$\dot{m}$	$[\text{kg s}^{-1}]$	mass flow rate
$P$	$[\text{€ kg}^{-1}]$	cost of individual chemicals
$t$	$[\text{s}]$	time
$\dot{V}$	$[\text{m}^3 \text{h}^{-1}]$	volume flow rate
$w$	$[\text{kg kg}^{-1}]$	weight fraction

## Greek letters

$\Delta$	$[-]$	difference
----------	-------	------------

## Sub- and superscripts

80	80 percent
active	active extraction part
C	carrier liquid
conti	continuous phase
dis	disperse phase
F	feed
flood	flooding
industrial	industrial system
model	model system
P	product
S	solvent
tot	total

## Abbreviations

DN	diamètre nominal
MC	measurement cell

## References

- [1] C. Hanson, *Recent Advances in Liquid-Liquid Extraction*, Elsevier Science, Burlington 1971.
- [2] H. W. Brandt, K.-H. Reissinger, J. Schröter, *Chem. Ing. Tech.* **1978**, 50 (5), 345–354. DOI: <https://doi.org/10.1002/cite.330500505>
- [3] A. Pfennig, J. Pilhofer, J. Schröter, *Fluidverfahrenstechnik*, 2nd ed., Wiley-VCH, Weinheim 2006.
- [4] S. Soboll, I. Hagemann, N. Kockmann, *Chem. Ing. Tech.* **2017**, 89 (12), 1611–1618. DOI: <https://doi.org/10.1002/cite.201700031>
- [5] S. Soboll, L. Bittorf, N. Kockmann, *Chem. Eng. Technol.* **2018**, 41 (1), 134–142. DOI: <https://doi.org/10.1002/ceat.201700152>
- [6] S. Soboll, N. Kockmann, *Chem. Eng. Technol.* **2018**, 41 (9), 1847–1856. DOI: <https://doi.org/10.1002/ceat.201800283>
- [7] T. Misek, R. Berger, J. Schröter, *Standard Test Systems for Liquid Extraction*, 2nd ed., European Federation of Chemical Engineering, Warwickshire 1985.
- [8] A. T. Laitinen, K. J. T. Penttilä, M. T. Manninen, J. K. Syrjänen, J. M. Kaunisto, L. S. Murtomäki, *Chem. Eng. Res. Des.* **2019**, 146, 518–527. DOI: <https://doi.org/10.1016/j.cherd.2019.04.018>
- [9] S. Mohanty, *Rev. Chem. Eng.* **2000**, 16 (3), 199–248. DOI: <https://doi.org/10.1515/REVCE.2000.16.3.199>
- [10] K. Belhamel, A. Hachemaoui, *J. Chem. Eng. Process. Technol.* **2017**, 08 (4), 1000356. DOI: <https://doi.org/10.4172/2157-7048.1000356>
- [11] A. Chouai, M. Cabassud, M. V. Le Lann, C. Gourdon, G. Casamatta, *Chem. Eng. Process. Process Intensif.* **2000**, 39 (2), 171–180. DOI: [https://doi.org/10.1016/S0255-2701\(99\)00086-0](https://doi.org/10.1016/S0255-2701(99)00086-0)
- [12] F. S. Mjalli, *Chem. Eng. Sci.* **2005**, 60 (1), 239–253. DOI: <https://doi.org/10.1016/j.ces.2004.07.117>
- [13] P. Kolb, Hydrodynamics and Mass Transfer in an Agitated Mini-plant Extractor Type Kühni, *PhD Thesis*, TU Kaiserslautern 2004.
- [14] G. P. Towler, R. K. Sinnott, *Chemical Engineering Design*, 6th ed., Elsevier, Amsterdam 2008.
- [15] R. E. Treybal, *Mass-Transfer Operations*, 3rd ed., McGraw-Hill, New York 1980.
- [16] K. Sattler, *Thermische Trennverfahren*, 3rd ed., VCH, Weinheim, Chichester 2001.
- [17] T. C. Frank, *Perry's Chemical Engineers' Handbook*, 8th ed., McGraw-Hill, New York 2008.
- [18] L. Steiner, *Rechnerische Erfassung der Arbeitsweise von flüssig-flüssig Extraktionskolonnen*, Vol. 154, VDI-Verlag, Düsseldorf 1988.
- [19] P. Häusler, Vergleichende Untersuchungen an gerührten Extraktionskolonnen, *PhD Thesis*, ETH Zürich 1985.
- [20] M. W. Hlawitschka, Computational Fluid Dynamics Aided Design of Stirred Liquid-Liquid Extraction Columns, *PhD Thesis*, TU Kaiserslautern 2013.
- [21] T. Steinmetz, Tropfenpopulationsbilanzgestütztes Auslegungsverfahren zur Skalierung einer gerührten Miniplant-Extraktionskolonne, *PhD Thesis*, TU Kaiserslautern 2007.